UC Irvine
UC Irvine Previously Published Works

Title

Lipid Rafts Reconstituted in Model Membranes

Permalink

Journal

ISSN

Authors

Dietrich, C
Bagatolli, LA
Volovyk, ZN
et al.

Publication Date

DOI

Copyright Information

Peer reviewed

Lipid Rafts Reconstituted in Model Membranes

C. Dietrich,* L. A. Bagatolli,[†] Z. N. Volovyk,[‡] N. L. Thompson,[‡] M. Levi,[§] K. Jacobson,[*,¶] and E. Gratton[†]

*Department of Cell Biology and Anatomy, [‡]Department of Chemistry, and [¶]Lineberger Comprehensive Cancer Center, University of North Carolina at Chapel Hill, Chapel Hill, North Carolina 27599, [†]Laboratory for Fluorescence Dynamics, Department of Physics, University of Illinois at Urbana-Champaign, Urbana, Illinois 61801, and [§]Department of Medicine, University of Texas Southwestern Medical Center at Dallas and Veterans Administration Medical Center, Dallas, Texas 75216 USA

ABSTRACT   One key tenet of the raft hypothesis is that the formation of glycosphingolipid- and cholesterol-rich lipid domains can be driven solely by characteristic lipid-lipid interactions, suggesting that rafts ought to form in model membranes composed of appropriate lipids. In fact, domains with raft-like properties were found to coexist with fluid lipid regions in both planar supported lipid layers and in giant unilamellar vesicles (GUVs) formed from 1) equimolar mixtures of phospholipid-cholesterol-sphingomyelin or 2) natural lipids extracted from brush border membranes that are rich in sphingomyelin and cholesterol. Employing headgroup-labeled fluorescent phospholipid analogs in planar supported lipid layers, domains typically several microns in diameter were observed by fluorescence microscopy at room temperature (24°C) whereas non-raft mixtures (PC-cholesterol) appeared homogeneous. Both raft and non-raft domains were fluid-like, although diffusion was slower in raft domains, and the probe could exchange between the two phases. Consistent with the raft hypothesis, GM1, a glycosphingolipid (GSL), was highly enriched in the more ordered domains and resistant to detergent extraction, which disrupted the GSL-depleted phase. To exclude the possibility that the domain structure was an artifact caused by the lipid layer support, GUVs were formed from the synthetic and natural lipid mixtures, in which the probe, LAURDAN, was incorporated. The emission spectrum of LAURDAN was examined by two-photon fluorescence microscopy, which allowed identification of regions with high or low order of lipid acyl chain alignment. In GUVs formed from the raft lipid mixture or from brush border membrane lipids an array of more ordered and less ordered domains that were in register in both monolayers could reversibly be formed and disrupted upon cooling and heating. Overall, the notion that in biomembranes selected lipids could laterally aggregate to form more ordered, detergent-resistant lipid rafts into which glycosphingolipids partition is strongly supported by this study.

INTRODUCTION

A current question in membrane biology and one whose answer could revolutionize our thinking about the lateral organization of membranes is whether glycosphingolipid-enriched domains (rafts) (Jacobson and Dietrich, 1999; Thompson and Tillack, 1985) exist in the plane of the natural membranes. This question has been prompted by the resistance of specialized lipid fractions and apically directed GPI-anchored proteins to extraction with cold non-ionic detergent (Brown and London, 1997; Brown and Rose, 1992) and has led to the hypothesis of specialized glyco-sphingolipid microdomains termed lipid rafts (Simons and Ikonen, 1997). If such domains exist, they would under-score the importance of lateral organization in biomembranes for complex activities such as signal transduction (Cinek and Horejsi, 1992) and membrane trafficking (Brown and Rose, 1992; Simons and van Meer, 1988). Because of potential artifacts inherent in detergent extrac-

tion, however, whether such domains actually exist in vivo remains controversial, although evidence is accumulating that suggests some form of these postulated structures represents reality.

The raft hypothesis proposes that certain naturally occurring lipids aggregate in the plane of the membrane driven solely by distinctive intermolecular interactions, including van der Waals interactions between the long, nearly fully saturated chains of sphingomyelin and glycosphingolipids as well as hydrogen bonding between adjacent glycosyl moieties of glycosphingolipids (Simons and Ikonen, 1997). The potential of glycosphingolipids to form domains was recognized earlier (Thompson and Tillack, 1985). Furthermore, the saturated nature of raft lipids and glycolipids acts to promote their interaction with cholesterol (Brown, 1998). All of these interactions are thought to underlie the detergent resistance of certain mixtures of lipids, particularly those containing sphingomyelin, cholesterol, glycosphingolipids, and saturated phospholipids. Indeed, the work of London, Brown and their co-workers indicated that liposomes formed from artificial raft lipid mixtures that mimic the composition of detergent-resistant membranes were partially resistant to detergent and showed spectroscopic evidence for a more ordered (raft) phase coexisting with a disordered phase in the plane of the membrane (Ahmed et al., 1997; Schroeder et al., 1994). Given this fact, it is important to determine whether such mixtures form visible, laterally extended domains in model membranes systems

and, if so, to measure the properties of such domains. Such data would form a baseline from which the properties of natural membrane raft domains could be compared.

Planar supported lipid layers constitute one model system that has the important advantage that bilayers may be constructed from two monolayers of different composition; thus, the inherent asymmetry of biological membranes may be mimicked. Despite the presence of the support, such lipid layers retain critical features such as the gel-to-liquid crystalline phase transition (Dietrich et al., 1997; Merkel et al., 1989; Tamm and McConnell, 1985). Giant unilamellar vesicles (GUVs) are a second model system that provides a free standing bilayer, without potential substrate effects. In such systems, domain structures occurring during phase transitions and phase separations can be visualized (Bagatolli and Gratton, 1999, 2000; Korlach et al., 1999).

MATERIALS AND METHODS

Commercial reagents

Egg phosphatidylcholine (egg-PC), 1,2-dipalmitoyl-*sn*-glycero-3-phosphocholine (DPPC), 1,2-dioleoyl-*sn*-glycero-3-phosphocholine (DOPC), 1-palmitoyl-2-oleoyl-*sn*-glycero-3-phosphocholine (POPC), cholesterol, brain sphingomyelin, and ovine ganglioside GM1 (GM1) were purchased from Avanti Polar Lipids (Birmingham, AL). Lipid samples were dissolved in chloroform (HPLC grade) at a concentration of 1 mg/ml for the preparation of planar supported lipid layers and at a concentration of ~0.2 mg/ml for the preparation of GUVs. The fluorescent lipid probes 1,2-dipalmitoyl-*sn*-glycero-3-phosphoethanolamine-fluorescein (FL-DPPE), 1,2-dipalmitoyl-*sn*-glycero-3-phosphoethanolamine-x-Texas Red (TR-DPPE), and 6-dodecanoyl-2-dimethylaminonaphthalene (LAURDAN) were obtained from Molecular Probes (Eugene, OR) whereas 1,2-dipalmitoyl-*sn*-glycero-3-phosphoethanolamine-*N*-(7-nitro-2–1,3-benzoxadiaxol-4-yl) (NBD-DPPE) was purchased from Avanti Polar Lipids; the probes were added to model membranes at a concentration of less than 1 mol % (see text). Fluorescein-conjugated cholera toxin B subunit (FL-CTB) was obtained from Sigma Chemical Co. (St. Louis, MO). Phosphate buffer saline (PBS) was prepared from 50 mM sodium phosphate, 150 mM NaCl, and 0.01% NaN$_3$. A purification system provided water with a specific resistance of 17.5 MΩ cm.

Lipid extraction from brush border membranes

Brush border membranes (BBMs) from the renal cortical tissue of adult Sprague Dawley rats were isolated and purified by the differential centrifugation and magnesium precipitation gradient method (Levi et al., 1987; Molitoris and Simn, 1985). Total lipids were extracted from BBMs by the method of Bligh and Dyer (Bligh and Dyer, 1959; Levi et al., 1987). To remove cholesterol, BBM total lipid extracts were fractionated using silicic acid columns (Superclean LC-Si SPE tubes, Supelco, Bellefonte, PA) washed with 2 ml of chloroform/methanol (1:1, v/v). Lipid extracts in 50 μl of chloroform/methanol (1:1) were loaded on the column. Cholesterol was eluted from the column with 5 ml of chloroform and discarded. Glycolipids were eluted with 20 ml of acetone. Phospholipids were eluted with 5 ml of methanol. The acetone and methanol fractions were combined and dried under nitrogen. Gas chromatographic analysis of cholesterol (Levi et al., 1985) revealed that >95% of the original cholesterol was removed by this method.

Preparation of planar supported phospholipid layers

Phospholipid bilayers were prepared by successive transfer of two lipid monolayers spread on the water-air interface of a Langmuir trough (32 dyne/cm) onto a glass coverslip as previously described (Merkel et al., 1989; Pisarchick and Thompson, 1990; Tamm and McConnell, 1985; Wright et al., 1988). Alternatively, instead of depositing the first phospholipid monolayer, the surface of the glass was silanized (Merkel et al., 1989; Tscharner and McConnell, 1981). For this procedure coverslips were exposed for 5 min to an argon ion plasma and then placed in a desiccator containing argon and a small dish of 0.5 ml of dimethyldichlorsilane (Sigma). A partial vacuum was applied to the desiccator for 1min. After 20 min the desiccator was again filled with argon. The silanized coverslips were held in a glass beaker covered with aluminum foil for up to 5 days. Before use, silanized coverslips were placed under a partial vacuum for at least 15 min.

Preparation of GUVs

GUVs were prepared by the electroformation method developed by Angelova and Dimitrov (Angelova et al., 1992; Angelova and Dimitrov, 1986) in a special temperature-controlled chamber, as previously described (Bagatolli and Gratton, 1999, 2000).

The LAURDAN labeling procedure was done in one of two ways. Either the fluorescent probe was premixed with the lipids in chloroform or a small amount (less than 1 μl) of LAURDAN in dimethylsulfoxide was added after the vesicle formation (0.5 mol %). The sample behavior during the temperature scan was independent of the labeling procedure. The GUV yield was approximately 95% and the mean diameter of the GUVs was ~40 μm. To check the lamellarity of the giant vesicles several vesicles labeled with LAURDAN were imaged using the two-photon excitation microscope. Intensities measured along the border of different vesicles in the liquid crystalline phase were very similar. Because the existence of multilamellar vesicles would give rise to different intensity images due to the presence of different numbers of LAURDAN-labeled lipid bilayers, it could be concluded that the vesicles were unilamellar (Bagatolli and Gratton, 1999, 2000; Bagatolli et al., 2000; Mathivet et al., 1996).

Imaging planar supported bilayers

Epifluorescence imaging of the planar supported lipid layers was done with an inverted microscope (Axiovert 10 with 100×/1.30 Plan-NeoFluar, Zeiss, Homldale, NJ) equipped with a CCD camera (MicroMax, 782 × 582 chip, Princeton Instruments, Trenton, NJ). All micrographs shown are 12-bit digitized images with 0.08-μm pixel resolution.

Single particle tracking

Single particle tracking (SPT) was conducted by binding 40-nm colloidal gold (BB International, Cardiff, UK) specifically to FL-DPPE embedded in planar supported monolayers. Control experiments revealed less than 5% nonspecific binding. Gold was imaged by means of computer-enhanced video microscopy described elsewhere (Lee et al., 1991). Video frames were recorded in video rate (30 frames/s) on the hard disk of a computer (O2, Silicon Graphics, Mountain View, CA) and were analyzed by the commercial software package ISEE (Inovision Corp., Durham, NC), which identifies relative changes of gold particle positions with an accuracy of a few nanometers ($\pm$8 nm). The diffusion coefficient D was obtained by calculating the squared displacement (SD = $dx^2 + dy^2$) of the particle positions (x, y) for different time intervals, dt. According to $\langle SD \rangle = 4D \times dt$ for a randomly diffusing particle in two dimensions, we obtained D by

fitting a line to the measured mean squared displacements $\langle SD \rangle$ for time intervals dt corresponding to one (33-ms) to three (100-ms) video frames.

Imaging GUVs

GUVs were imaged and measured using a scanning two-photon excitation microscope developed in the Laboratory for Fluorescence Dynamics (Parasassi et al., 1991; So et al., 1996) and employing an X20 LD-Achroplan (0.4 NA) long-working-distance objective (Zeiss). To change the polarization of the laser light from linear to circular, a quarter wave-plate (CVI Laser Corp., Albuquerque, NM) was used. The fluorescence emission was observed through a broad band-pass filter from 350 to 600 nm (BG39 filter, Chroma Technology, Brattleboro, VT). A miniature photomultiplier (R5600-P, Hamamatsu, Bridgewater, NJ) was used for light detection in the photon-counting mode. The diameters of the vesicles were measured using size-calibrated fluorescent spheres as a standard (latex FluoSpheres, polystyrene, blue fluorescent 360/415, diameter 15.5 μm, Molecular Probes). The pixel size in these experiments was 0.52 μm.

Generalized polarization

To quantify LAURDAN emission spectrum changes, the excitation generalized polarization (GP) was used, defined in analogy to fluorescence polarization, as:

$$GP = \frac{I_B - I_R}{I_B + I_R},$$

where I_B and I_R correspond to the intensities at the blue and red edges, respectively, of the emission spectrum using a given excitation wavelength (Parasassi et al., 1990, 1991). The LAURDAN GP for the GUV images was computed on a pixel by pixel basis using two LAURDAN fluorescence images, one obtained in the blue (I_B) and the other obtained in the green (I_R) regions of the LAURDAN emission spectrum (Bagatolli and Gratton, 1999, 2000; Parasassi et al., 1997; Yu et al., 1996). To obtain these images, two additional optical band-pass filters centered at (446 $\pm$ 23) nm (I_B) and at (499 $\pm$ 23) nm (I_R) (Ealing Electro-Optics, Holliston, MA) were used sequentially in the emission path of the microscope.

RESULTS AND DISCUSSION

Fig. 1 shows, schematically, the model membrane systems employed in this study. Planar supported phospholipid monolayers and bilayers are shown in Fig. 1, *a* and *b*, respectively. In Fig. 1 *a*, the distal lipid monolayer (bright lipid heads) is supported on a silanized glass substrate. In Fig. 1 *b*, the layer proximate to the glass substrate (dark heads) is a phospholipid monolayer of a composition that can be the same or different from that of the distal phospholipid monolayer. As indicated, fluorescent lipid probes were added only to the lipid mixture forming the distal monolayer. A GUV is depicted in Fig. 1 *c* (*right*) with the close-up illustrating the position of LAURDAN within the freestanding, undisturbed phospholipid bilayer. GUVs prepared by electroformation are typically tens of microns in diameter.

Fig. 2 *a* shows the molecular structure of the various fluorescent lipid analogs employed. LAURDAN is known to be embedded in the hydrophobic region of a phospholipid bilayer partitioning equally between liquid crystalline and gel phases (Bagatolli and Gratton, 1999, 2000; Parasassi et al., 1990). The emission spectrum is sensitive to the degree of alignment of acyl chains within the bilayers, and therefore this probe can be used to identify lipid phases. The three fluorescent phospholipid analogs employed in the planar supported phospholipid layer experiments were selected to visualize coexistence of lipid phases on the basis of different probe partitioning into ordered or disordered regions. To illustrate the differential partitioning of the three probe molecules into ordered gel domains, we employed DPPC monolayers on the water-air interface as a well studied model system (McConnell, 1991; Möhwald, 1990).
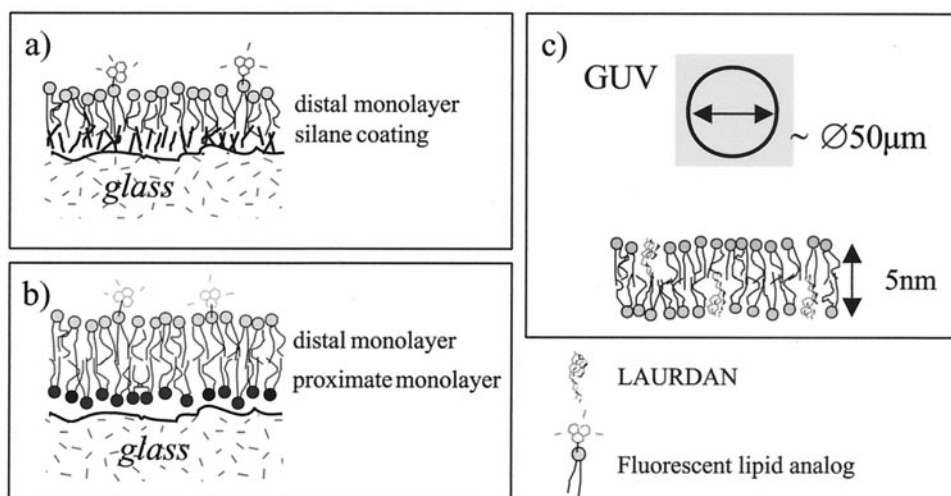

FIGURE 1 Schematic diagram of model membrane systems employed. (*a* and *b*) Phospholipid monolayers with added fluorescent lipid analogs deposited onto silanized glass (*a*) or another lipid monolayer that is supported by the glass substrate (*b*). (*c*) Giant unilamellar vesicle (GUV) (*top*) with magnified section (*bottom*) showing bilayer and embedded LAURDAN probes.
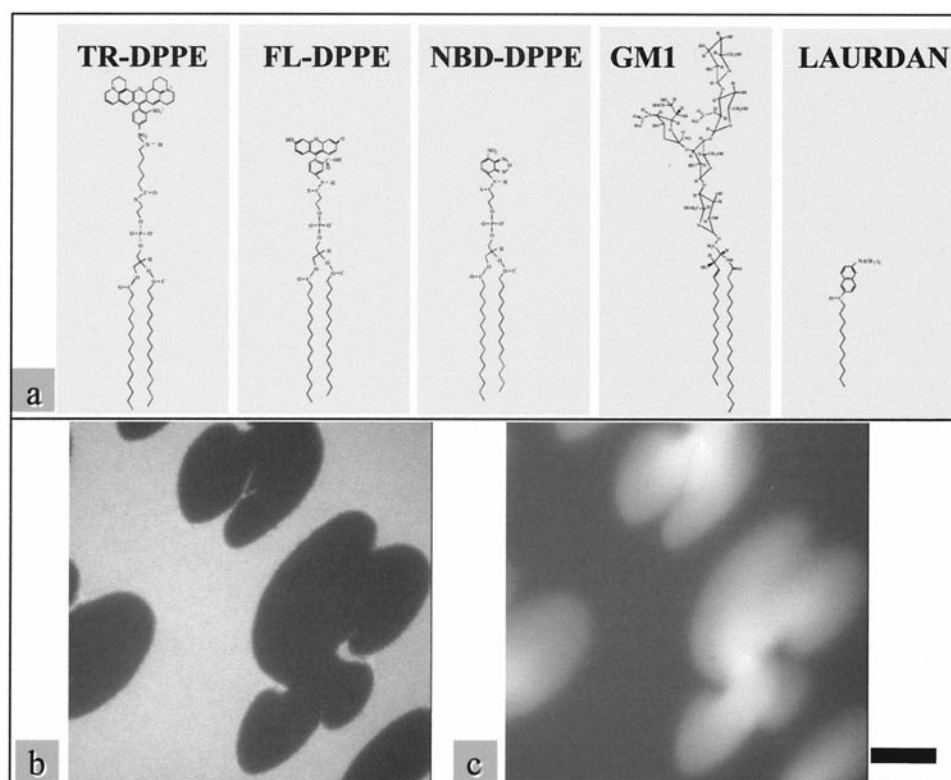
FIGURE 2 (*a*) Chemical structures of the various fluorescent lipid analogs employed and the glycosphingolipid, GM1; (*b* and *c*) Micrographs showing fluorescence of distal DPPC monolayer (with 0.5 mol % TR-DPPE and 1 mol % GM1) observed in rhodamine channel (*b*) and fluorescein channel (*c*). The distal DPPC monolayer was deposited in the coexistence region for liquid and gel phases at 8 dyne/cm and 24°C from the water-air interface, to a proximal DPPC monolayer that was transferred previously to a glass coverslip at 32 dyne/cm. To stain GM1, the sample was incubated with FL-CTB (1 μg/ml in PBS) for 10 min. Bar, 20 μm.

At room temperature and a lateral pressure of a few dynes/cm, DPPC forms gel-like domains with a very characteristic propeller-like shape (Weis and McConnell, 1984) that coexist with a surrounding fluid crystalline phase. Although TR-DPPE (Fig. 2 *b*) and FL-DPPE (not shown) probes are largely excluded from the gel domains that appear dark, NBD-DPPE (not shown) and GM1 (Fig. 2 *c*) partition significantly into the propeller-like domains, indicating an affinity for more ordered phases.

Supported lipid monolayers

Raft monolayers deposited on alkylated glass substrata show clear domain formation. If DOPC (not shown), POPC (not shown), DOPC/cholesterol (2/1) (not shown), POPC/cholesterol (2:1) (Fig. 3 *a*) and raft mixtures composed of DOPC/cholesterol/sphingomyelin (1/1/1) (not shown) or POPC/cholesterol/sphingomyelin (2:1:1) (Fig. 3 *b*) are compared, coexistence of two lipid phases is seen only in the raft monolayers. Usually domains several microns in diameter were observed, from which TR-DPPE (not shown) and FL-DPPE (Fig. 3 *b*) were largely excluded whereas NBD-DPPE (not shown) significantly partitioned into these do-

mains. The tendency for TR-DPPE and FL-DPPE to be excluded both from the ordered DPPC propeller phase (Fig. 2 *b*) and the domains (Fig. 3 *b*) suggests that the latter are more ordered.

Complete fluorescence recovery after photobleaching (FRAP) conducted with NBD-DPPE and FL-DPPE was observed for both lipid phases, indicating that they were both fluid-like (data not shown). We applied single particle tracking (SPT), observing the movement of single gold particles (Ø 40 nm) that were specifically attached to FL-DPPE. Separately recorded fluorescence images allowed identification of regions depleted or enriched with the fluorescent lipid analog. We selected the particles that switched during a recording between the two phases and therefore allowed us to directly compare the lipid probe mobility in the two phases for the same particle. An example where the particle switched several times between the two phases is shown in Fig. 3 *c*. Separating and analyzing (see Materials and Methods) the jump length statistics for all particles (five), we found that their diffusion coefficient was reduced by a factor of ~2 when entering regions that preferentially excluded FL-DPPE. This small decrement in lateral diffusion coefficient in one phase is consistent with
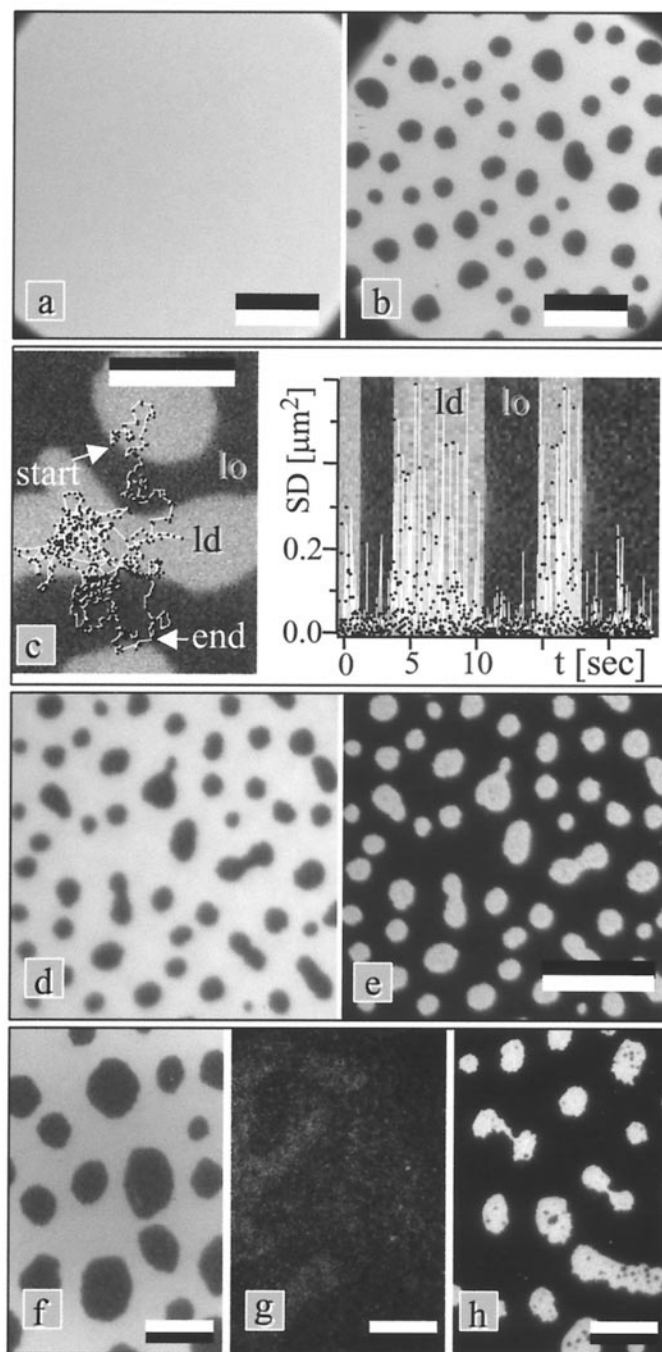
FIGURE 3   Fluorescence micrographs of phospholipid monolayers supported by silanized glass substrates at room temperature (see Materials and Methods). (*a*) Non-raft mixture (POPC/cholesterol 2:1); (*b*) Raft-mixture (POPC/cholesterol/sphingomyelin 2:1:1). Both contain 0.5 mol % FL-DPPE. (*c*, *left panel*) DOPC/cholesterol/sphingomyelin 1:1:1) containing 0.5 mol % FL-DPPE and 1 mol % GM1 with overlaid trajectory of gold particle (Ø 40 nm) as visualized by SPT (Saxton and Jacobson, 1997). Gold was functionalized to bind specifically to FL-DPPE lipid analogs that are enriched in the liquid-disordered (*ld*) lipid phase and appear bright in the fluorescence image while being depleted from the liquid-ordered (*lo*) phase (see text). (*Right panel*) Squared jump distance (SD) between successive video frames ($dt = 33$ ms) for a trajectory. The fluorescence image permitted separation between parts of the particle trajectory pertaining to the two different lipid phases. Trajectory analysis (see Materials and Methods) for this particle yielded $D_{ld} = 1.1 \times 10^{-8}$ cm^2/s and $D_{lo} = 0.38 \times 10^{-8}$ cm^2/s. (*d* and *e*) Double-stained POPC/cholesterol/sphingomyelin (2:1:1) phospholipid monolayer containing 1 mol % GM1 and 0.1 mol % TR-DPPE after a 10-min incubation with FL-CTB (1 μg/ml in PBS) as observed in rhodamine channel (*d*) and fluorescein channel (*e*). (*f–h*) DOPC/cholesterol/sphingomyelin (1:1:1) containing 1 mol % GM1 with 0.5 mol % FL-DPPE as observed in fluorescein channel, before (*f*) and after (*g*) a 30-min incubation with detergent solution (0.2% Triton X-100 in PBS); *h* shows sample after a post-extraction incubation with FL-CTB (1 μg/ml in PBS for 10 min). With the exception of *c* (5 μm), all scale bars are 10 μm. All experiments were conducted at room temperature (24°C).

earlier work showing that increasing cholesterol content in lipid mixtures causes reductions in D of approximately twofold (Almeida et al., 1992; Ladha et al., 1996; Tanaka et al., 1999; Wu et al., 1977). These results suggest that this class of domains is in a second phase that is a cholesterol-rich, liquid-ordered phase.

Glycosphingolipids are thought to be an important component of lipid rafts in cell membranes. To study the distribution of a prototypical glycosphingolipid, the ganglioside GM1 was added to the phospholipid mixtures at 1 mol %. Again, the formation of domains was observed only for raft monolayers; the presence of GM1 caused no noticeable changes in either partitioning of the fluorescent lipid analogs or domain shape compared with GM1-free monolayers. To visualize the glycosphingolipids, samples were incubated with FL-CTB, which binds specifically to GM1. Fig. 3 *e* shows that GM1 clearly resides in the more ordered domains, whereas TR-DPPE lies outside these regions (Fig. 3 *d*). By contrast, the distribution of 1 mol % GM1 in POPC or POPC/cholesterol was uniform as visualized by FL-CTB staining (not shown).

Because lipid rafts are hypothesized to be detergent resistant, the effect of detergent extraction (30 min of 0.2% Triton X-100 in PBS at room temperature) on the planar supported raft-lipid monolayers was studied. TR-DPPE (not shown) and FL-DPPE (Fig. 3 *f*), which both reside in the less ordered lipid phase, were readily extracted by the

detergent treatment (Fig. 3 *g*). In contrast, GM1 (stained with FL-CTB after detergent extraction) was still detected in the more ordered domains (Fig. 3 *h*), indicating these regions were detergent resistant.

Supported lipid bilayers

To provide a more realistic model of biological membranes, egg-PC monolayers were first deposited on glass followed by deposition of monolayers having the raft lipid composition. This system also exhibited clear micron-sized, oval domains, independent of addition of GM1 (1 mol %). TR-DPPE (Fig. 4 *a*) was largely excluded from the domains, FL-DPPE (Fig. 4 *b*) was distributed nearly equally between the two phases whereas NBD-DPPE (Fig. 4 *c*) and GM1, after labeling with FL-CTB (Fig. 4 *d*), were found to be enriched in domains as judged by fluorescence intensities. The preparations shown in Fig. 4 *a* and *d*, were double stained for TR-DPPE and FL-CTB, respectively. Interestingly, GM1 in the plasma membrane, when labeled with FL-CTB, is also found in an aggregated state (Stauffer and Meyer, 1997).

Both lipid phases contain mobile molecules because photobleaching a large area shows that recovery leads to repopulation of both phases, as shown for NBD-DPPE in Fig. 4 *e*. This effect can be seen because the oval domains are
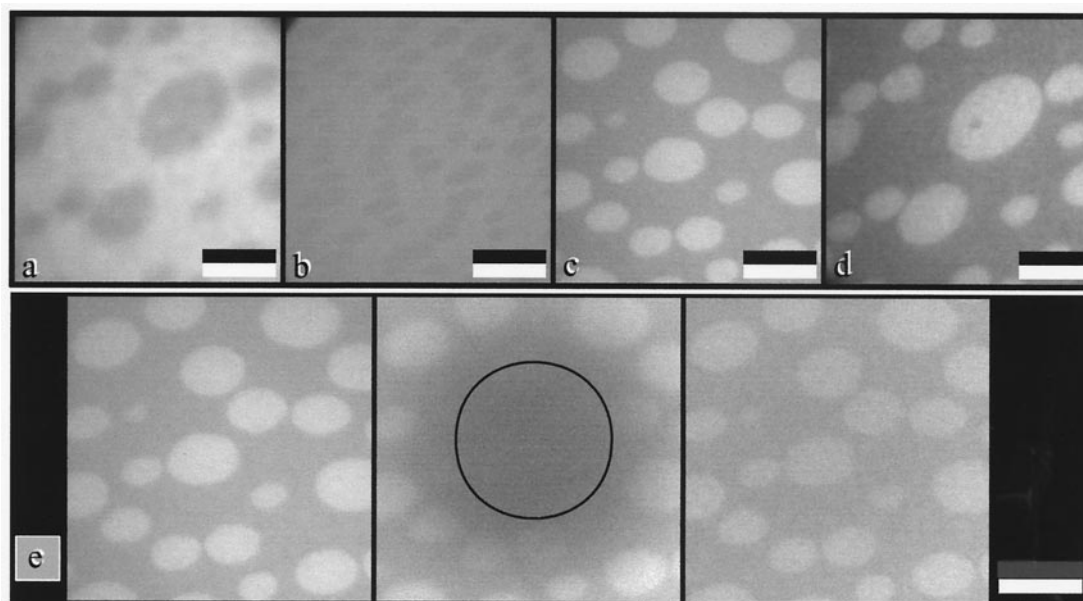

FIGURE 4 Fluorescence micrographs of planar supported phospholipid bilayers made from POPC/cholesterol/sphingomyelin (2:1:1) with 1 mol % GM1 (distal to glass support) and egg PC (proximate to glass support). Only distal lipid layers contain fluorescent lipid dyes. (*a*) 0.1 mol % TR-DPPE; (*b*) 0.5 mol % FL-DPPE; (*c*) 0.5 mol % NBD-DPPE; (*d*) FL-CTB. Note that images *a* and *d* were obtained from the same bilayer preparation, which was double labeled with TR-DPPE and FL-CTB (for 10 min at 1 μg/ml in PBS). Bars, 10 μm. (*e*) Fluorescence from NBD-DPPE equilibrates between liquid-ordered and liquid-disordered regions: (*left*) before photobleaching; (*middle*) after 4 min of continuous photobleaching; (*right*) after 4 min of recovery. The circle in the central panel indicates the size of the field stop during the bleaching period. To achieve a significant bleaching rate, neutral density filters in the illumination path of the HBO100 were removed during bleaching. Bar, 10 μm. All images were recorded at room temperature (24°C).

spatially stable and do not drift laterally in the outer mono-layer, making it possible to observe fluorescence recovery within identified domains. It is plausible that the solid glass support, which is not flat on the molecular scale, will cause epitaxial coupling that affects the overlaying lipid molecules (see Fig. 1, *a* and *b*). Rädler et al. (1995) interpreted the roughness observed at the edge of a lipid bilayer spreading on a hydrophilic surface to be caused by substrate defects. These could be envisioned as extending glass peaks that act as pinning centers for the fluid-fluid phase border. The mobility results indicate that molecules are translationally mobile in both phases, that there is an exchange of molecules between the two fluid phases, and that the energy barrier between these two types of regions is relatively low.

GUVs

One possible artifact of planar supported monolayers and bilayers is that the substrate may influence the structure of the layers. For this reason, the behavior of unsupported GUVs constructed from raft lipid mixtures was examined. Such bilayers were labeled with LAURDAN, a probe that is sensitive to the water content within the bilayer and thus to the ordering of acyl chains (Bagatolli and Gratton, 1999, 2000; Parasassi and Gratton, 1995; Parasassi et al., 1998). In particular, the emission of LAURDAN can be red-shifted by as much as 50 nm in the liquid-disordered phase relative to the gel phase due to solvent dipole relaxation during the excited-state lifetime of the probe. Furthermore, when the

excitation light is linearly polarized, clear photoselection effects occur dependent on the orientation of the LAUR-DAN transition dipole moments with respect to 1) the plane of polarization and 2) the phase state of the bilayer (Bagatolli and Gratton, 1999, 2000; Parasassi et al., 1997). The first effect means that certain regions of a spherical bilayer are preferentially excited. The second effect leads to increased excitation in a fluid bilayer, even for unfavorable polarization conditions, because of rotational freedom of the LAURDAN probe.

Domains on the order of 10 μm in dimension were seen in polar sections of the raft lipid GUVs by scanning two-photon fluorescence microscopy as the vesicles were cooled through 25°C (Fig. 5). The formation of these domains was not altered by addition of 1 mol % GM1, and domains were not seen in GUVs formed from non-raft lipids. If the lipid domains were larger than the image pixel size and circularly polarized excitation light was used, more and less ordered lipid domains in the top of the vesicle were differentiated because photoselection renders the more ordered domains less fluorescent and the less ordered domains more fluorescent. Because the probe is located in both bilayers, raft domains are co-localized in the outer and inner leaflets of GUVs and inter-bilayer coupling occurs at least in a free-standing bilayer composed of raft lipids. This phenomenon has been seen in earlier studies for gel-like domains present in GUVs of binary phospholipid mixtures (Bagatolli and Gratton, 2000; Korlach et al., 1999). The domains could be reversibly formed and disrupted by repeated cooling and
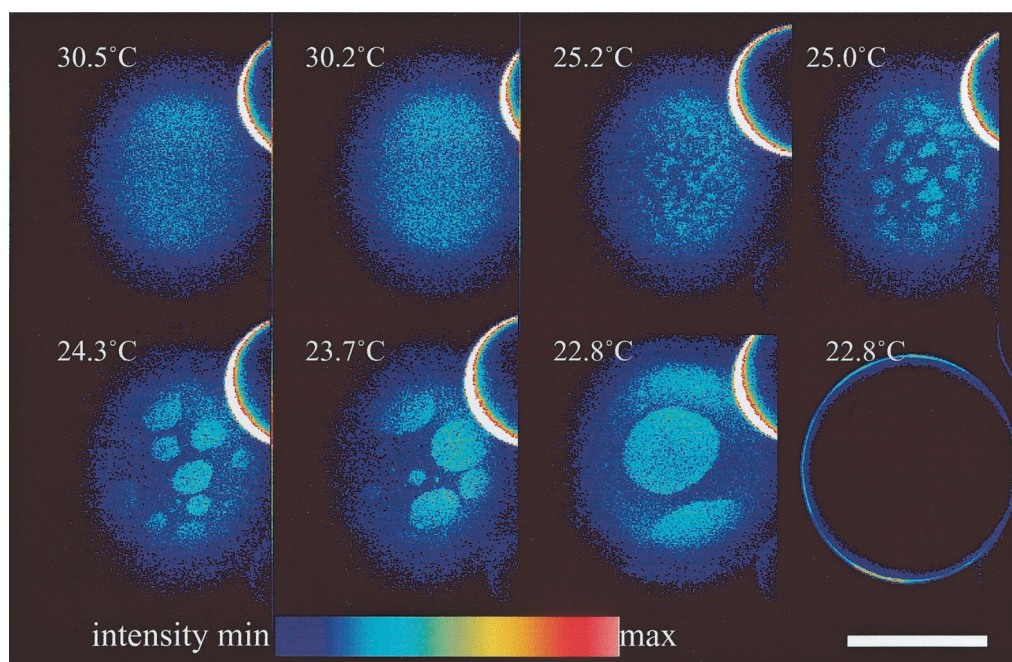

FIGURE 5 Two-photon excitation fluorescence intensity images (false color representation) of LAURDAN-labeled GUV as a function of temperature formed from DOPC/cholesterol/sphingomyelin (1:1:1) with 1 mol % GM1 added. The images have been taken at the top part of the GUV. The lower right panel shows an equatorial section demonstrating the absence of internal vesicles. Bar, 50 μm.

heating (data not shown). The lower right panel shows an equatorial section at 22.8°C and indicates the absence of internal vesicles that could complicate interpretation of the results.

Several lines of evidence indicate the coexistence of two fluid phases. First, the perfectly round shape of domains found in GUVs indicates that they are in a fluid-phase state. When fluid domains are embedded in a fluid environment, circular domains will form because both phases are isotropic and the line energy (tension), which is associated with the rim of two demixing phases, is minimized by optimizing the area-to-perimeter ratio. Second, inspection of two images separated by 1 min shows that dark domains (black arrows) and bright domains (white arrows) moved relative to each other, indicating that the two phases in which they were embedded were fluid (Fig. 6, *a* and *b*). Additional evidence for the coexistence of two phases is given in Fig. 6, *c* and *d*. In addition to the photoselection effect, the less ordered domains have a red-shifted emission compared with the more ordered domains. Thus, when the emission was viewed selectively with a longer-wavelength interference filter centered at 490 nm (Fig. 6 *c*), the less ordered domains appeared much more intense than when viewed with a shorter-wavelength filter centered at 440 nm (Fig. 6 *d*). Note that in polar sections of GUVs the transition dipole of LAURDAN in the ordered phase is oriented perpendicular to the polarization of the incident laser light, and therefore LAURDAN in this phase does not appreciably contribute to the fluorescence signal. Finally, because LAURDAN is homogeneously distributed between solid and fluid phospholipid phases (Bagatolli and Gratton, 1999, 2000; Parasassi and Gratton, 1995; Parasassi et al., 1998), the generalized polarization (GP) recorded from equatorial sections of the GUVs, where all LAURDAN may be excited, can be used to discriminate between more ordered (high GP) and less ordered (low GP) domains as shown in Fig. 6 *e*. The GP histogram (Fig. 6 *f*) must be fitted with a bimodal distribution, because fluorescence images indicate the coexistence of two phases with different GP values. Note that the values in the two bimodal GP distributions fall between the GP values for gel-phase DPPC and liquid-crystalline-phase DPPC (Fig. 6 *f*), suggesting the coexistence of a more ordered and less ordered fluid phase.

Model membranes formed from BBM lipids

The composition of the raft lipids is believed to be a good approximation to that found in detergent-resistant membranes (Schroeder et al., 1994). To check this assumption, it was of interest to examine GUVs formed from natural membrane lipid extracts. The brush border of the proximal renal tubule is rich in sphingomyelin and glycosphingolipids and has a very high cholesterol-to-phosphate-containing lipid ratio (0.85) (Levi et al., 1987). Therefore, this membrane might be expected to be a rich source of putative rafts.
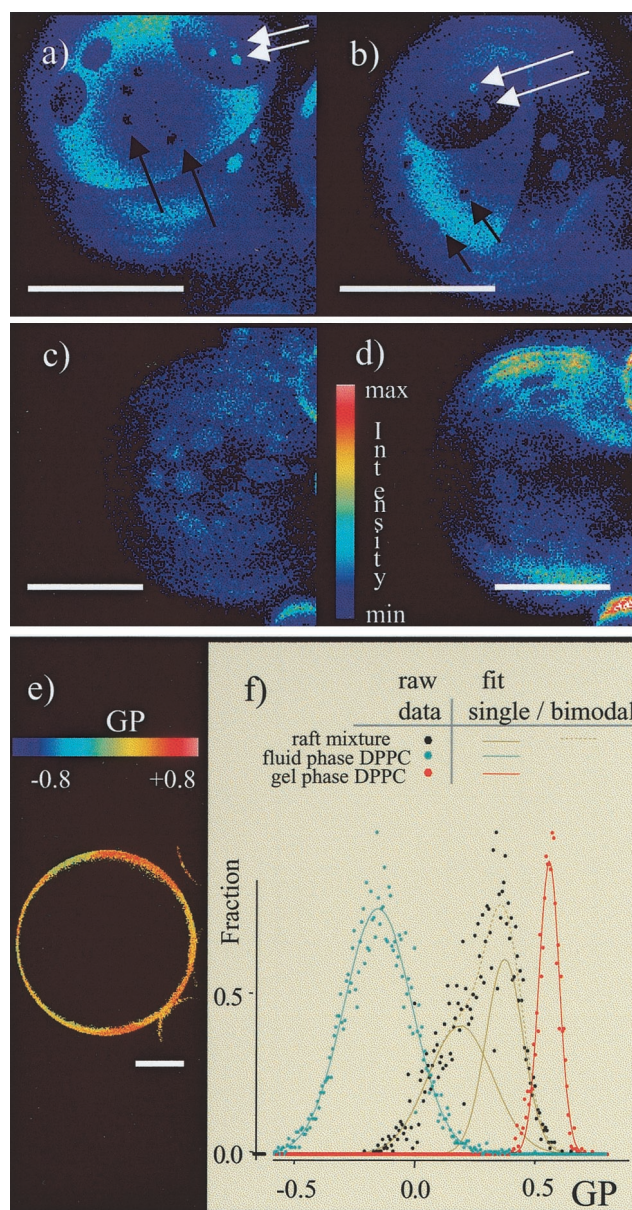

FIGURE 6   (*a* and *b*) Two-photon excitation fluorescence intensity images (false color representation) of LAURDAN-labeled GUVs at 16°C taken 1 min apart. GUVs were formed from DOPC/cholesterol/sphingomyelin (1:1:1) with 1 mol % GM1 added. The images have been taken at the top part of the GUV. (*c* and *d*) Two-photon excitation LAURDAN intensity images at 24.6°C taken at the top of a single GUV composed of DOPC/cholesterol/sphingomyelin (1:1:1) with 1 mol % GM1. (*c*) Image with 490 ± 23 nm interference filter in place; (*d*) Image with 440 ± 23 nm interference filter in place; (*e* and *f*) GP image of equatorial section of GUV composed of raft mixture and corresponding GP histogram (*f*), which is fit to bimodal distribution. For reference, GP histograms with single-component fits of pure gel phase DPPC (red) and pure liquid crystalline DPPC (blue) are included. Scale bars, 50 μm.

Indeed, GUVs formed from such lipids also showed round domains (Fig. 7 *a*) of large dimension. Moreover, these domains formed upon cooling to 45°C, indicating a remarkable stability. However, in contrast to GUVs formed from
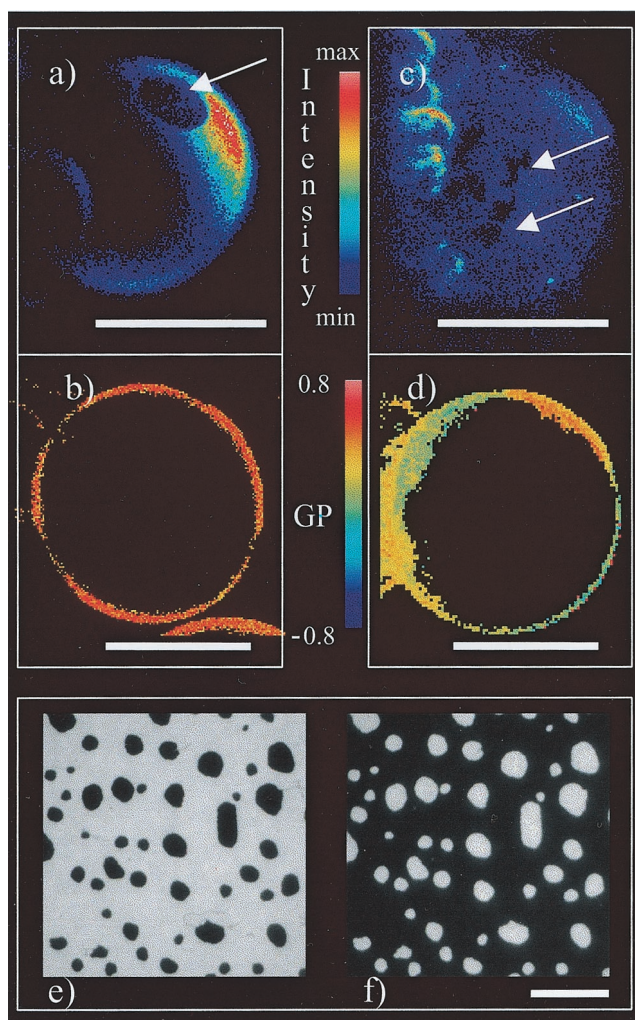
FIGURE 7 Two-photon fluorescence images of polar sections (*a* and *c*) and GP images of equatorial sections (*b* and *d*) of LAURDAN-labeled GUV formed from extracted brush border membrane lipids with cholesterol present (*a* and *b*) at 28°C or with cholesterol extracted (*c* and *d*) at 15°C (see Materials and Methods). Bars, 50 μm. (*e* and *f*) Planar supported BBM monolayer with 0.2 mol % TR-DPPE and 1 mol % GM1 after incubation with FL-CTB (1 μg/ml in PBS for 15 min) as observed in rhodamine channel (*e*) and fluorescein channel (*f*). Bar for planar supported lipid layer is 10 μm.

raft lipid mixtures, the domains in GUVs formed from the natural lipid extracts showed no detectable LAURDAN emission in either polar or equatorial sections. This result implies either that the LAURDAN probe is excluded from the domains or that the fluorescence is nearly completely quenched in these domains. Consequently the GP images recorded in the equatorial sections of GUVs (Fig. 7 *b*) appear single colored, and the GP histograms were well fit with single-component distributions (single Gaussian fit, data not shown) reflecting the loss of emission from one class of domains. The perfectly round shape of the domains (arrow in Fig. 7 *a*) was a good indication that they were formed from a fluid-like phase as discussed above.

If cholesterol was removed (>95%) from the BBM lipid extracts, domain formation in GUV was inhibited until cooling to 24°C when domains start to form. Their shape was highly irregular (Fig. 7 *c*, arrows) similar to gel domains observed in the fluid-gel coexistence region of binary phospholipid mixtures (Bagatolli and Gratton, 1999, 2000; Korlach et al., 1999); this result suggests that a sphingomyelin-enriched gel-like phase occurs in the absence of cholesterol. GP images of equatorial sections of vesicles showed different color segments along the vesicle contour (Fig. 7 *d*), indicating that LAURDAN was present in both lipid phases, similar to that observed for gel-fluid coexistence in other model systems (Bagatolli and Gratton, 1999, 2000). This observation was confirmed by the GP histograms, which were well fitted only when assuming a two-component distribution (double Gaussian fit, data not shown). Above 24°C vesicles appeared homogeneous in two-photon fluorescence and the GP histograms were well fit by a single-component distribution (single Gaussian fit).

BBM lipids also formed domains in planar supported monolayers deposited on silanated glass substrates. TR-DPPE was excluded from these domains (Fig. 7 *e*). Significant staining of these domains with FL-CTB occurred only when GM1 (1 mol %) was added to the BBM lipids (Fig. 7 *f*). This indicates that the added GM1 partitions into the more ordered phase. The results with BBM lipids demonstrate that formation of fluid-phase coexistence is not restricted to synthetic mixtures, containing only few lipid species, but may exist in a natural multi-component lipid mixture. It is important to note that this natural lipid mixture was not defined by its detergent insolubility.

Domain formation in model membranes

In GUVs, domain formation and growth were clearly controlled by temperature. For planar supported phospholipid layers, however, the final equilibrium was established within a few seconds after the first layer was pushed through the second monolayer at the air/water interface. Consequently, for these layers the size and shape of domains varied considerably. Even for GUVs, we found significant variations in domain patterns between different experiments (see Figs. 5 and 6). This indicates that the growth, shape, and size of domains depends critically on experimental parameters that are difficult to control, such as impurities, exact lipid compositions, and the specific path and speed taken to equilibrium. In planar supported model membranes, domains were usually formed by the liquid-ordered phases, as judged by probe partitioning and GM1 enrichment (Figs. 3 and 4). However, in nearly every preparation, regions were present with a reversed contrast where domains were formed by the liquid-disordered phase. Sometimes domains were enclosed in domains, which themselves were embedded in the coexisting phase, very much as shown in Fig. 6, *a* and *b*, for a GUV. In contrast to

planar supported lipid layers, lowering the temperature in GUVs induced in most samples the formation of liquid-disordered domains as judged by the measured GP values. These observations suggest that, for the lipid mixtures investigated, the phase coexistence region is entered near a critical point, where the two forming lipid phases differ little in their composition. Overall the experiments establish that the coexistence of two fluid liquid-crystalline phases in a lipid bilayer may not be limited to the formation of highly unstable and dynamic domains comprising only several hundreds of molecules, but rather this coexistence can consist of macroscopic domains, very similar to those observed in the coexistence of gel and liquid-crystalline phases (Bagatolli and Gratton, 2000; Korlach et al., 1999).

Cellular implications

Domain size in natural membranes

Domain formation, size, and shape depended critically on various experimental conditions in model systems but typically domains grew to dimensions 10 μm or more for the lipid mixtures employed. In biomembranes, clearly there are factors that limit the size of rafts to considerably smaller dimensions than can occur in the model membranes (for review see Jacobson and Dietrich, 1999). There are physical and biological arguments why domains should be much smaller in biological membranes. To have very large rafts would seem to negate the effectiveness of rafts as a dispersed, regulatory structure. In natural membranes, nucleation and/or fusion processes could be under cellular control. Specifically, it is likely that the membrane-associated cytoskeleton would play a major role both in regulating raft size (Jacobson and Dietrich, 1999) and in laterally positioning rafts. There is a remarkably large proportion of lipids present with the potential to form rafts in the plasma membrane so that detergent-resistant domains cover a large fraction of the cell surface (Mayor and Maxfield, 1995). This suggests that more subtle regulatory factors are involved in providing much smaller domains with appropriate functionality. It is plausible that the physiological conditions found in cells provide an environment that keeps the membrane matrix close to a coexistence region, allowing domain formation and growth to be triggered by small changes in lipid composition or by delivering molecules that act as nucleation centers for raft formation (Brown and London, 1998).

Partitioning into raft domains

In addition to the cellular regulation of raft size and shape, the partitioning of molecules in and out of rafts is presumably another important aspect of regulation possibly involving post-translational modifications and/or expression levels as well as cross-linking of molecules (Brown and London,

1998; Harder and Simons, 1997; Sheets et al., 1999). The relative partitioning of probe molecules into the DPPC propeller (Fig. 2, b and c) and raft domains (Fig. 4, a–d) is similar. Because acyl chain alignment/order is high for these two phases, this finding is in line with the interpretation that the tendency for a probe molecule to partition into these phases is driven by the preference to be within an ordered acyl-chain environment. However, it is striking that changes in the headgroup of various lipid analogs employed with identical acyl chain structure produced dramatic differences in partitioning between coexisting liquid-ordered and liquid-disordered phases. This result can be explained by the fact that at the head attached dyes can significantly interact with the hydrophobic or interfacial region of the lipid/water interface (Asuncion-Punzalan et al., 1998) affecting the organization of acyl chains. These results suggest the structure of the juxtamembrane region of membrane components could affect how raft domains are populated by selected molecular species.

Transbilayer coupling

Some insights into the issue of transbilayer coupling and its potential role in transmembrane signal transduction may be garnered from this study. In GUVs, raft domains in either monolayer are in register, suggesting that under certain conditions, raft domains in the outer monolayer of the plasma membrane have the potential to aggregate selected lipids in the inner monolayer; this feature could provide a mechanism for how raft receptors in the outer monolayer are coupled to cytoplasmic components of signal transduction pathways, a question that has eluded simple answers (Brown and London, 1998).

Conclusion

Overall, the properties of domains in various model systems reproduce many of the properties expected for lipid rafts in vivo including the coexistence of liquid-ordered and liquid-disordered phases and the ability of the more ordered phase to concentrate glycosphingolipids and resist detergent extraction. These results lend strong support to the notion that much smaller lipid rafts, whose size is regulated by various biological factors, could exist in biomembranes driven by the tendency of certain lipids to strongly interact in the plane of the membrane.

REFERENCES

Ahmed, S. N., D. A. Brown, and E. London. 1997. On the origin of sphingolipid/cholesterol-rich detergent-insoluble cell membranes: phys-

iological concentrations of cholesterol and sphingolipid induce formation of a detergent-insoluble, liquid-ordered lipid phase in model membranes. *Biochemistry.* 36:10944–10953.

Almeida, P. F., W. L. C. Vaz, and T. E. Thompson. 1992. Lateral diffusion in the liquid-phases of dimyristoylphosphatidylcholine cholesterol lipid bilayers: a lateral diffusion free-volume analysis. *Biochemistry.* 31: 6739–6747.

Angelova, M. L., and D. S. Dimitrov. 1986. Liposome electroformation. *Faraday Discuss. Chem. Soc.* 81:303–311.

Angelova, M. I., S. Soléau, P. Meléard, J. F. Faucon, and P. Bothorel. 1992. Preparation of giant vesicles by external AC fields. Kinetics and application. *Prog. Colloid Polymer Sci.* 89:127–131.

Asuncion-Punzalan, E., K. Kachel, and E. London. 1998. Groups with polar characteristics can locate at both shallow and deep locations in membranes: the behavior of dansyl and related probes. *Biochemistry.* 37:4603–4611.

Bagatolli, L. A., and E. Gratton. 1999. Two photon fluorescence microscopy observation of shape changes at the phase transition in phospholipid's giant unilamellar vesicles. *Biophys. J.* 77:2090–2101.

Bagatolli, L. A., and E. Gratton. 2000. Two-photon fluorescence microscopy of coexisting lipid domains in giant unilamellar vesicles of binary phospholipid mixtures. *Biophys. J.* 78:290–305.

Bagatolli, L. A., T. Parasassi, and E. Gratton. 2000. Giant phospholipid vesicles: comparison among the whole lipid sample characteristics using different preparation methods. A two photon fluorescence microscopy study. *Chem. Phys. Lipids.* 105:135–147.

Bligh, E. G., and W. J. Dyer. 1959. A rapid method of total lipid extraction and purification. *Can J. Biochem. Physiol.* 37:911–917.

Brown, R. E. 1998. Sphingolipid organization in biomembranes: what physical studies of model membranes reveal. *J. Cell Sci.* 111:1–9.

Brown, D. A., and E. London. 1997. Structure of detergent-resistant membrane domains: does phase separation occur in biological membranes? *Biochem. Biophys. Res. Commun.* 240:1–7.

Brown, D. A., and E. London. 1998. Function of lipid rafts in biological membranes. *Annu. Rev. Cell Dev. Biol.* 14:111–136.

Brown, D. A., and J. Rose. 1992. Sorting of GPI-anchored proteins to glycolipid enriched membrane subdomains during transport to the apical cell surface. *Cell.* 68:533–544.

Cinek, T., and V. Horejsi. 1992. The nature of large noncovalent complexes containing glycosyl-phosphatidylinositol-anchored membrane glycoproteins and protein tyrosine kinases. *J. Immunol.* 149:2262–2270.

Dietrich, C., R. Merkel, and R. Tampé. 1997. Diffusion measurement of fluorescence-labeled amphiphilic molecules with a standard fluorescence microscope. *Biophys. J.* 72:1701–1710.

Harder, T., and K. Simons. 1997. Caveolae, DIGs, and the dynamics of sphingolipid-cholesterol microdomains. *Curr. Opin. Cell Biol.* 9:534–542.

Jacobson, K., and C. Dietrich. 1999. Looking at lipid rafts? *Trends Cell Biol.* 9:87–91.

Korlach, J., P. Schwille, W. W. Webb, and G. W. Feigenson. 1999. Characterization of lipid bilayer phases by confocal microcopy and fluorescence correlation spectroscopy. *Proc. Natl. Acad. Sci. U.S.A.* 96:8461–8466.

Ladha, S., A. R. Mackie, L. J. Harvey, D. C. Clark, E. J. A. Lea, M. Brullemans, and H. Duclohier. 1996. Lateral diffusion in planar lipid bilayers: a fluorescence recovery after photobleaching investigation of its modulation by lipid composition, cholesterol, or alamethicin content and divalent cations. *Biophys. J.* 71:1364–1373.

Lee, G. M., A. Ishiara, and K. Jacobson. 1991. Direct observation of Brownian motion of lipids in a membrane. *Proc. Natl. Acad. Sci. U.S.A.* 88:6274–6278.

Levi, M., D. M. Jameson, and W. B. van de Meer. 1985. Role of BBM lipid composition and fluidity in impaired renal Pi transport in aged rat. *Am. J. Physiol.* 256:F85–F94.

Levi, M., B. A. Molitoris, T. J. Burke, R. W. Schrier, and F. R. Simon. 1987. Effects of vitamin D-induced chronic hypercalcemia on rat renal

cortical plasma membranes and mitochondria. *Am. J. Physiol.* 252: F267–F275.

Mathivet, L., S. Cribier, and P. F. Devaux. 1996. Shape change and physical properties of giant phospholipid vesicles prepared in the presence of an AC electric field. *Biophys. J.* 70:1112–1121.

Mayor, S., and F. R. Maxfield. 1995. Insolubility and redistribution of GPI-anchored proteins at the cell surface after detergent treatment. *Mol. Biol. Cell.* 6:929–944.

McConnell, H. M. 1991. Structures and transitions on lipid monolayers at the water air interface. *Annu. Rev. Phys. Chem.* 42:171–195.

Merkel, R., E. Sackmann, and E. Evans. 1989. Molecular friction and epitactic coupling between monolayers in supported bilayers. *J. Phys. (France).* 50:1535–1555.

Möhwald, H. 1990. Phospholipid and phospholipid-protein monolayers at the air/water interface. *Annu. Rev. Phys. Chem.* 117:269–280.

Molitoris, B. A., and F. R. Simn. 1985. Renal cortical brush border and basolateral membranes: cholesterol and phospholipid composition and relative turnover. *J. Membr. Biol.* 83:207–215.

Parasassi, T., and E. Gratton. 1995. Membrane lipid domains and dynamics detected by LAURDAN. *J. Fluoresc.* 5:59–70.

Parasassi, T., E. Gratton, W. Yu, P. Wilson, and M. Levi. 1997. Two photon fluorescence microscopy of LAURDAN generalized polarization domains in model and natural membranes. *Biophys. J.* 72:2413–2429.

Parasassi, T., E. Krasnovska, L. A. Bagatolli, and E. Gratton. 1998. LAURDAN and PORDAN as polarity sensitive fluorescent membrane probes. *J. Fluoresc.* 8:365–373.

Parasassi, T., G. D. Stasio, A. d'Ubaldo, and E. Gratton. 1990. Phase fluctuation in phospholipid membranes revealed by LAURDAN fluorescence. *Biophys. J.* 57:1179–1186.

Parasassi, T., G. D. Stasio, D. Ravagnan, R. M. Rusch, and E. Gratton. 1991. Quantitation of lipid phases in phospholipid vesicles by the generalized polarization of LAURDAN fluorescence. *Biophys. J.* 60: 179–189.

Pisarchick, M. L., and N. L. Thompson. 1990. Binding of a monoclonal antibody and its Fab fragment to supported phospholipid monolayers measured by total internal reflection fluorescence microscopy. *Biophys. J.* 58:1235–1249.

Rädler, J., H. Strey, and E. Sackmann. 1995. Phenomenology and kinetics of lipid bilayer spreading on hydrophilic surfaces. *Langmuir.* 11: 4539–4545.

Saxton, M. J., and K. Jacobson. 1997. Single-particle tracking: applications to membrane dynamics. *Annu. Rev. Biophys. Biomol. Struct.* 26: 373–399.

Schroeder, R., E. London, and D. A. Brown. 1994. Interactions between saturated acyl chains confer detergent resistance on lipids and glycosylphosphatidylinositol (GPI)-anchored proteins: GPI-anchored proteins in liposomes and cells show similar behavior. *Proc. Natl. Acad. Sci. U.S.A.* 91:12130–12134.

Sheets, E. D., D. Holowka, and B. Baird. 1999. Membrane organization in immunoglobulin E receptor signaling. *Curr. Opin. Chem. Biol.* 3:95–99.

Simons, K., and E. Ikonen. 1997. Functional rafts in cell membranes. *Nature.* 387:569–572.

Simons, K., and G. van Meer. 1988. Lipid sorting in epithelial cells. *Biochemistry.* 27:6197–6202.

So, P. T. C., T. French, W. M. Yu, K. M. Berland, C. Y. Dong, and E. Gratton. 1996. Two-photon fluorescence microscopy: time-resolved and intensity imaging. *In* Fluorescence Imaging Spectroscopy and Microscopy, Chemical Analysis Series, Vol. 137. X. F. Wang and B. Herman, eds. John Wiley & Sons, Inc., New York. 351–374.

Stauffer, T. P., and T. Meyer. 1997:Compartmentalized IgE receptor-mediated signal transduction in living cells. *J. Cell Biol.* 139:1447–1454.

Tamm, L. K., and H. M. McConnell. 1985. Supported phospholipid bilayers. *Biophys. J.* 47:105–113.

Tanaka, K., P. A. Manning, V. K. Lau, and H. Yu. 1999. Lipid lateral diffusion in dilauroylphosphatidylcholine/cholesterol mixed monolayers at the air/water interface. *Langmuir.* 15:600–606.

Thompson, T. E., and T. W. Tillack. 1985. Organization of glycosphingo-lipids in bilayers and plasma membrane of mammalian cells. *Annu. Rev. Biophys. Biophys. Chem.* 14:361–386.

Tscharner, V., and H. M. McConnell. 1981. Physical properties of lipid monolayers on alkylated planar glass surfaces. *Biophys. J.* 36:421–427.

Weis, R. M., and H. M. McConnell. 1984. Two-dimensional chiral crystals of phospholipid. *Nature.* 310:47–49.

Wright, L. L., A. G. Palmer, and N. L. Thompson. 1988. Inhomogeneous translational diffusion of monoclonal antibodies on phospholipid Lang-muir-Blodgett films. *Biophys. J.* 54:463–470.

Wu, E.-S., K. Jacobson, and D. Papahadjopoulos. 1977. Lateral diffusion in phospholipid multibilayers measured by fluorescence recovery after photobleaching. *Biochemistry.* 16:3936.

Yu, W., P. T. So, T. French, and E. Gratton. 1996. Fluorescence general-ized polarization of cell membranes: a two-photon scanning microscopy approach. *Biophys. J.* 70:626–636.